Low Band Gap Donor−Acceptor Conjugated Polymers toward Organic Solar Cells Applications

Kristof Colladet,[†] Sofie Fourier,[†] Thomas J. Cleij,[†] Laurence Lutsen,[‡] Jan Gelan,[†] and Dirk Vanderzande*[,†,‡]

Institute for Materials Research (IMO), Hasselt University, Agoralaan, Building D, B-3590 Diepenbeek, Belgium, and Division IMOMEC, IMEC, Wetenschapspark 1, B-3590 Diepenbeek, Belgium

Le Huong Nguyen, Helmut Neugebauer, and Serdar Sariciftci

Linz Institute for Organic Solar Cells (LIOS), Johannes Kepler University, Altenbergerstr. 69, A-4040 Linz, Austria

Aranzazu Aguirre, Griet Janssen, and Etienne Goovaerts

Physics Department, University of Antwerp, Universiteitsplein 1, B-2610 Antwerpen, Belgium

Received August 3, 2006; Revised Manuscript Received November 8, 2006

ABSTRACT: Mixtures of conjugated polymers and fullerenes command considerable attention for application in organic solar cells. To increase their efficiency, the design of new materials that absorb at longer wavelengths is of substantial interest. We have prepared such low band gap polymers using the donor−acceptor route, which is based on the concept that the interaction between alternating donors and acceptors results in a compressed band gap. Furthermore, for application in photovoltaic devices, sufficient polymer solubility is required. We have prepared four low band gap conjugated polymers, with a bis(1-cyano-2-thienylvinylene)phenylene base structure, and achieved an excellent solubility by the introduction of long alkoxy and alkyl side chains. The polymers were synthesized via an oxidative polymerization. Their electronic properties were determined from electrochemical and optical measurements, which confirm that they indeed have a low band gap. In the blend of such a low band gap polymer with PCBM, evidence for efficient charge transfer was obtained from PL and EPR measurements. However, bulk heterostructure solar cells made of such blends display only low efficiencies, which is attributed to low charge carrier mobilities.

I. Introduction

Interpenetrating networks of conjugated polymers and buckminsterfullerene (C_{60}) are receiving increasing attention in the field of thin film organic solar cells.[1−4] In these devices an ultrafast photoinduced charge transfer takes place between the conjugated polymer as donor and the fullerene as acceptor. A large interfacial area in the active layer is required since the exciton diffusion length in polymers is only nanometers long, and the charge transfer takes place at the donor−acceptor interface. In the second step the charges are transported to and collected at the electrodes. Power efficiencies of 2.9% were reported for bulk heterojunction solar cells made of poly-[2-(3,7-dimethyloctyloxy)-5-methyloxy]-*p*-phenylenevinylene (MDMO−PPV) and [6,6]-phenyl C_{61} butyric acid methyl ester (PCBM).[5] Since one of the limiting parameters for photovoltaic energy conversion is the mismatch of the absorption spectrum of the active layer and the solar emission, the optical band gap of the polymer used is of crucial importance for increasing the efficiency. Polymers with band gaps above 2 eV only absorb in the ultraviolet (UV) and the green part of the visible range. Radiation at long wavelengths (>600 nm) passes through the solar cell and makes little contribution to the photocurrent. Therefore, the design of new materials that absorb at higher wavelengths is an ongoing issue for synthetic chemists.[6−9] Recently, efficiencies of 5.2% were reported for solar cells consisting of regioregular poly(3-hexylthiophene-2,5-diyl) (P3HT) and PCBM.[10] One of the reasons for this spectacular increase, besides an optimized morphology and device preparation, is the lower band gap of P3HT (2.0 eV) as compared to MDMO−PPV (2.2 eV). It is clear now that specific electronic properties of the polymer are necessary, and in this aspect the ability to fine-tune the energy levels of the valence band (VB) and conduction band (CB), and hence the band gap (E_g), is of growing interest. One of the most promising strategies to tailor the energy levels of conjugated polymers is the donor−acceptor route.[11] The central concept forming the basis of this route is that the interaction between alternating electron-rich donors and electron-deficient acceptors will result in a compressed band gap. Furthermore, by changing the substituents of the polymer, the band gap can be fine-tuned. Various literature reports exist in which this method is used to electrosynthesize low band gap polymers containing cyanovinylene spacers as the acceptor units and thiophene derivatives as the donor. Band gaps ranging from 1.1 to 1.6 eV were reported.[12−15] However, for photovoltaic devices soluble low band gap polymers are needed since the conjugated polymer must be blended with a complementary acceptor to achieve a bulk heterojunction. One possibility toward solubility is the use of a precursor route toward low band gap polymers.[8,16] A drawback of this method is that precursor polymers undergo a further conversion in thin film which can deteriorate the quality of the film and thus the device performance. Another possibility to make conjugated polymers soluble is to introduce long flexible side chains as reported here.

* Corresponding author: Ph +32 (0)11 26 83 21; Fax +32 (0)11 26 83 01; e-mail dirk.vanderzande@uhasselt.be.
[†] Hasselt University.
[‡] IMEC.

10.1021/ma061760i CCC: $37.00
Published on Web 12/13/2006

In this work we present a family of four conjugated polymers based on bis(1-cyano-2-thienylvinylene)phenylene. The structure consists of a central dialkoxyphenylene core (donor) para-disubstituted by two thiophene derivatives (donor) through a cyanovinylene linker (acceptor). By changing the thiophene moiety, we were able to tune the polymers electronic and solubility properties. Moreover, our approach to keep the central core constant leads to a toolbox to create a whole range of monomers, and thus polymers, with different heteroaromatic rings linked to this central core. The polymers were synthesized via oxidative polymerization with $FeCl_3$.[17] Up until now, other direct synthetic pathways toward low band gap materials were either very difficult to handle or yielded only relatively low molecular weight polymers. On the other hand, the $FeCl_3$ method is a well-established method to polymerize thiophene-like monomers and continues to be the most widely used and straightforward method to prepare polythiophene derivatives. In this work, our main goal was to synthesize soluble, high molecular weight polymers and compare their electronic and solar cell characteristics.

II. Experimental Section

Chemicals. All reagents and chemicals were obtained from commercial sources (Acros, Aldrich, and Merck) and used without further purification, unless otherwise stated. 3,4-Ethylenedioxythiophene, distilled under reduced pressure prior to use, and poly(3,4-ethylenedioxythiophene):poly(styrenesulfonate) (PEDOT:PSS) (Baytron P) were provided by Bayer AG. 2-Tetradecyl-2,3-dihydrothieno[3,4-*b*][1,4]dioxin was kindly donated by Agfa-Gevaert N.V. Tetrahydrofuran (THF), acetonitrile, and chloroform were dried by distillation from sodium/benzophenone, CaH_2, and P_2O_5 respectively. Commercial $FeCl_3$ was purified and treated to obtain anhydrous $FeCl_3$[18] and was stored in a Schlenk-type flask under an inert atmosphere. 1,4-Bischloromethyl-2,5-bis[3′,7′-dimethyloctyl)oxy]benzene (**1**), 3-octyl-2-thienylaldehyde (**4**), 3,4-ethylenedioxy-2-thienylaldehyde (**5**), and 3- or 4-tetradecyl-2,3-dihydrothieno[3,4-*b*][1,4]dioxine-5-carbaldehyde (**6**) were synthesized according to procedures previously reported.[15,19]

Instrumentation. NMR spectra were recorded on a Varian Inova 300 spectrometer at 300 MHz for ^1H NMR and at 75 MHz for ^{13}C NMR using a 5 mm probe. ^1H and ^{13}C chemical shifts are reported in ppm downfield from tetramethylsilane (TMS) reference using the residual protonated solvent resonance as an internal standard. Melting points (uncorrected) were measured on an Electrothermal IA9100 digital melting point apparatus. Gas chromatography/mass spectrometry (GC/MS) analyses were carried out on TSQ-70 and Voyager mass spectrometers (Thermoquest); the capillary column was a Chrompack Cpsil5CB or Cpsil8CB. DIP-MS measurements were performed at a heating rate of 10 °C/min up to 600 °C. In this technique the material is brought directly on the heating element of the probe as a thin film, and this enables to study the products that are liberated in the high vacuum (4×10^{-4} Pa) inside the spectrometer. Liberated products were ionized by electron impact. Elemental analysis was performed with a Flash EA 1112 series CHNS-O analyzer. Analytical size exclusion chromatography (SEC) was performed using a Spectra series P100 (Spectra Physics) pump equipped with two mixed-B columns (10 μm, 2 × 30 cm, Polymer Labs) and a refractive index detector (Shodex) at 40 °C. THF was used as the eluent at a flow rate of 1.0 mL/min. Molecular weight distributions are given relative to polystyrene standards. Unless stated otherwise, all thin films in the following characterization methods were prepared by spin-coating from a $CHCl_3$ solution (10 mg/mL). UV−vis spectroscopy was performed on a Varian CARY 500 UV−vis−NIR spectrophotometer. Samples for thin film UV−vis characterization were prepared by spin-coating the polymer onto quartz disks. For temperature-dependent thin film UV−vis characterization the disks were heated in a Harrick high-temperature cell (heating rate: 2 °C/min), which was positioned in the beam of the UV−vis spectrometer to allow in-situ measurements. Spectra were taken continuously under a continuous flow of N_2, during which the samples were in direct contact with the heating element. Thin film electrochemical properties were measured with an Eco Chemie Autolab PGSTAT 20 potentiostat/galvanostat using a conventional three-electrode cell (electrolyte: 0.1 mol/L $TBAPF_6$ in anhydrous CH_3CN) with an Ag/Ag^+ reference electrode (0.01 mol/L $AgNO_3$, 0.1 mol/L $TBAPF_6$, and CH_3CN), a platinum counter electrode, and a platinum wire as working electrode. Cyclic voltammograms were recorded at 50 mV/s under a N_2 atmosphere, and all potentials were referenced using a known internal standard ferrocene/ferrocinium, which in acetonitrile solution is estimated to have an oxidation potential of −4.98 eV vs vacuum. The polymers were directly spin-coated onto the Pt working electrode. A Varian Cary Eclipse fluorometer was used for the photoluminescence (PL) measurements. Time-resolved PL spectra were obtained by streak camera detection after excitation with 400 nm laser pulses (1.5 kHz, <2 ps) from the frequency-doubled output of a Ti-sapphire laser amplifier (Spectra Physics Spitfire). These experiments were performed on solutions of either the pure polymer or a mixture of the polymer and PCBM in a 1:1 ratio by weight and on spin-coated films (thickness ∼100 nm) prepared from these solutions. A Bruker ELEXSYS E680 spectrometer in conjunction with a split-coil 6 T superconducting magnet was used for W-band (95 GHz) light-induced electron paramagnetic resonance (LI-EPR). These measurements were performed at 100 K using an Oxford flow cryostat and with a Bruker cylindrical cavity which allows optical access to the sample via an optical fiber. Optical excitation was performed with the 488 nm line of an Ar^+ laser. The results presented here are recorded with a modulation frequency and amplitude of 100 kHz and 3 G, respectively, and a microwave frequency and microwave power of 94.0795 GHz and 0.07 mW. The samples were prepared from dried drop-cast films of the 1:1 ratio polymer/PCBM solution. Using the bulk heterojunction concept, photovoltaic devices were fabricated from a blend of the polymer as a donor and PCBM as an acceptor. A solution of the polymer and PCBM in a 1:2 ratio (by weight) was prepared in chloroform with a total concentration of 10 mg/mL. Poly(3,4-ethylenedioxythiophene):poly(styrenesulfonate) (PEDOT:PSS) (Baytron P) was spin-coated on top of an indium−tin oxide (ITO) coated glass (∼25 Ω/sq) which had been cleaned in an ultrasonic bath with acetone and isopropyl alcohol. Then the active layer (polymer:PCBM blend) was spin-coated on the PEDOT:PSS layer (about 80 nm thick). 6 Å of lithium fluoride (LiF) and 80 nm thick Al electrode were deposited on the blend film by thermal evaporation at $\sim 5 \times 10^{-6}$ mbar. Device annealing was carried out inside a glovebox at 120 °C for 4 min. All current−voltage ($I-V$) characteristics of the photovoltaic devices were measured using a Keithley SMU 2400 unit under inert atmosphere (argon) in a dry glovebox. A Steuernagel solar simulator under AM 1.5 conditions was used as the excitation source with an input power of 100 mW cm^{-2} white light illumination. A lock-in technique was used to measure the incident photon-to-current efficiency (IPCE). With this technique the number of electrons produced from the cell under short-circuit conditions is related to the number of incident photons. Light intensity correction was performed using a calibrated Si photodiode. The hole mobility of the polymers was measured in thin film field effect transistor (TF-FET) devices. The measurements were performed on a top-contact parallel transistor ($L = 60$ μm, $W = 9000$ μm). It consisted of a highly doped Si substrate on which an isolating oxide (SiO_2) of 100 nm was grown thermally on one side and of which the backside was covered with an aluminum layer as gate electrode. The polymers were spin-coated on top of the oxide. Subsequently, the gold contacts (source and drain) were evaporated on top of the device.

Synthesis. 1,4-Biscyanomethyl-2,5-bis[3′,7′-dimethyloctyl)oxy]-benzene (2). Finely crushed sodium cyanide (8.0 g, 0.164 mol) and 1,4-bischloromethyl-2,5-bis[3′,7′-dimethyloctyl)oxy]benzene (**1**) (20 g, 0.041 mol) are dissolved in 100 mL of anhydrous DMF. This mixture is heated at 110 °C for 1 h. After cooling, the mixture is poured in 150 g of crushed ice, upon which a brown solid precipitates. The solid is collected via filtration and washed on the

filter with hexane. Recrystallization from hexane yields an off white solid (15.9 g, 83% yield; mp 83−84 °C). ^{1}H NMR ($CDCl_3$): 6.90 (s, 2H), 4.00 (m, 4H), 3.67 (s, 4H), 1.80 (m, 2H), 1.52 (m, 6H), 1.29−1.15 (m, 12H), 0.92 (d, 6H), 0.85 (d, 12H). ^{13}C NMR ($CDCl_3$): 149.82, 118.85, 117.68, 112.37, 67.08, 39.04, 37.08, 36.01, 29.69, 27.80, 24.52, 22.54, 22.45, 19.51, 18.49. GC MS (EI, *m*/*e*): 468 (M^+), 328 ($M^+ - C_{10}H_{20}$), 188 ($M^+ - 2 \times C_{10}H_{20}$).

2-(4-(1-Cyano-2-thiophen-2-ylvinyl)-2,5-bis(3,7-dimethyloctyloxy)phenyl)-3-thiophen-2-ylacrylonitrile (M1). A mixture of **2** (5 g, 11 mmol) and 2-thiophenecarboxaldehyde (2.9 g, 26 mmol) is dissolved in 50 mL of MeOH. Sodium *tert*-butoxide (10 g, 110 mmol) is added as a solid, and this mixture is stirred for 24 h at reflux temperature. Upon cooling, a bright yellow solid (3.3 g, 46% yield) precipitates, which is filtered and washed with cold methanol; mp 109−110 °C. ^{1}H NMR ($CDCl_3$): 8.00 (s, 2H), 7.64 (d, 2H), 7.54 (d, 2H), 7.14 (t, 2H), 7.10 (s, 2H), 4.08 (m, 4H), 1.89 (m, 2H), 1.58 (m, 6H), 1.30−1.10 (m, 12H), 0.93 (d, 6H), 0.82 (d, 12H). ^{13}C NMR ($CDCl_3$): 150.53, 138.80, 138.15, 130.12, 129.82, 127.80, 124.05, 118.37, 114.09, 104.67, 67.91, 39.17, 37.29, 36.27, 29.88, 27.91, 24.69, 22.67, 22.51, 19.51. DIP MS (EI, *m*/*e*): 656 (M^+), 375 ($M^+ - 2 \times C_{10}H_{20}$). Anal. Calcd for $C_{40}H_{52}N_2O_2S_2$: C 73.13; H 7.98; N 4.26; O 4.87; S 9.76. Found: C 73.26; H 8.38; N 4.01; O 5.03; S 8.85. UV−vis (film) λ_{max}: 344, 407 nm.

2-(4-(1-Cyano-2-(3-octylthiophen-2-yl)-vinyl)-2,5-bis(3,7-dimethyloctyloxy)phenyl)-3-(3-octylthiophen-2-yl)acrylonitrile (M2). Monomer **M2** is prepared in an analogous way as described for **M1**. Starting from **2** (1 g, 2 mmol), 3-octyl-2-thienylaldehyde (**4**) (1.1 g, 5 mmol) and sodium *tert*-butoxide (2 g, 20 mmol). After cooling, 50 mL of water is added, and the mixture is extracted three times with 50 mL of CH_2Cl_2. The organic layer is dried over $MgSO_4$, and the solvent evaporated. **M2** is obtained as a sticky oil. After purification by column chromatography (silica, $CHCl_3$/*n*-hexane 1/1) a yellow oil is obtained (1.1 g, 60% yield). ^{1}H NMR ($CDCl_3$): 8.10 (s, 2H), 7.45 (d, 2H), 7.13 (s, 2H), 6.60 (d, 2H), 4.08 (m, 4H), 2.70 (t, 4H), 1.86 (m, 2H), 1.72−1.42 (br, m, 8H), 1.38−1.00 (br, m, 36H), 0.96−0.74 (br, m, 24H). ^{13}C NMR ($CDCl_3$): 150.39, 148.62, 144.08, 137.67, 131.89, 128.88, 124.36, 118.63, 114.08, 102.98, 68.03, 39.07, 37.17, 36.19, 31.72, 31.06, 29.75, 29.32, 29.12, 28.81, 27.80, 24.52, 22.52 (8C), 19.47, 13.96. DIP MS (EI, *m*/*e*): 881 (M^+) 600 ($M^+ - 2 \times C_{10}H_{20}$). Anal. Calcd for $C_{56}H_{84}N_2O_2S_2$: C 76.31; H 9.61; N 3.18; O 3.63; S 7.28. Found: C 76.46; H 10.11; N 3.01; O 3.32; S 6.61. UV−vis (film) λ_{max}: 337, 392 nm.

2-(4-(1-Cyano-2-(3,4-ethylenedioxythiophen-2-yl)vinyl)-2,5-bis(3,7-dimethyloctyloxy)phenyl)-3-(3,4-ethylenedioxythiophen-2-yl)acrylonitrile (M3). Monomer **M3** is prepared in an analogous way as described for **M1**. Starting from **2** (8 g, 17 mmol), 3,4-ethylenedioxy-2-thienylaldehyde (**5**) (6.4 g, 38 mmol), and sodium *tert*-butoxide (16.3 g, 170 mmol), **M3** is obtained as a bright orange solid (8.3 g, 63% yield), which is filtered and washed with methanol; mp 157−158 °C. ^{1}H NMR ($CDCl_3$): 8.16 (s, 2H), 7.07 (s, 2H), 6.59 (s, 2H), 4.28 (m, 4H), 4.23 (m, 4H), 4.06 (m, 4H), 1.86 (m, 2H), 1.67 (m, 6H), 1.30−1.10 (m, 12H), 0.92 (d, 6H), 0.82 (d, 12H). ^{13}C NMR ($CDCl_3$): 150.46, 144.24, 141.33, 134.61, 123.82, 118.94, 114.16, 113.90, 104.95, 101.19, 67.87, 65.10, 64.49, 39.21, 37.20, 36.24, 29.70, 27.93, 24.57, 22.68, 22.55, 19.61. DIP MS (EI, *m*/*e*): 772 (M^+), 632 ($M^+ - C_{10}H_{20}$), 491 ($M^+ - 2 \times C_{10}H_{20}$). Anal. Calcd for $C_{44}H_{56}N_2O_6S_2$: C 68.36; H 7.30; N 3.62; O 12.42; S 8.30. Found: C 68.76; H 7.51; N 3.88; O 11.85; S 8.04. UV−vis (film) λ_{max}: 348, 425 nm.

2-(4-(1-Cyano-2-(3- or 4-tetradecyl-2,3-dihydrothieno[3,4-*b*]-(1,4)dioxin-5-yl)vinyl)-2,5-bis(3,7-dimethyloctyloxy)phenyl)-3-(3- or 4-tetradecyl-2,3-dihydrothieno[3,4-*b*](1,4)dioxin-5-yl)-acrylonitrile (M4). Monomer **M4** is prepared in an analogous way as described for **M2**. Starting from **2** (1 g, 2 mmol), 3- or 4-tetradecyl-2,3-dihydroyhieno[3,4-*b*][1,4]dioxine-5-carbaldehyde (**6**) (1.7 g, 5 mmol), and sodium *tert*-butoxide (2 g, 20 mmol), **M4** is obtained as a sticky oil. After purification by column chromatography (silica, $CHCl_3$/*n*-hexane 9/1) a yellow-orange oil is obtained (1.7 g, 72% yield). ^{1}H NMR ($CDCl_3$): very complex mixture of four isomers and thus very difficult to analyze in detail.[20] Anal. Calcd for $C_{72}H_{112}N_2O_6S_2$: C 74.18; H 9.68; N 2.40; O 18.23; S 5.50. Found: C 74.64 H 9.90; N 2.06; O 8.33; S 4.89. DIP MS (EI, *m*/*e*): 1165 (M^+). UV−vis (film) λ_{max}: 334, 397 nm.

Table 1. Polymerization Results for Polymers P1−P4

	time [h]	M_w[a]	M_n[a]	PD[a]	Y1[b] [%]	Y2[c] [%]
P1	24	136 000	53 000	2.5	52	26
	48	32 000	5 500	5.8	24	35
	72	18 000	5 600	3.1	22	57
P2	24	35 000	15 000	2.3	82	91
	48	43 000	7 000	6.2	28	80
	72	7 900	2 500	3.2	30	85
P3	24	199 000	65 000	2.9	56	20
	48	33 000	7 700	4.3	31	43
	72	33 000	10 000	3.3	37	41
P4	24	40 000	14 000	3.0	76	82
	48	21 000	7 000	3.0	14	90
	72	24 000	3 500	6.7	18	93

[a] Determined by means of SEC in THF using polystyrene standards. [b] Overall yield. [c] Soluble polymer yield with respect to the overall yield.

General Procedure of Polymerization. The polymers are prepared by chemical oxidation of the monomers using $FeCl_3$ according to a procedure similar to that of Sugimoto et al.[17] Anhydrous $FeCl_3$ (4 mmol) is suspended in 50 mL of dry $CHCl_3$ under an Ar atmosphere, to which a solution of the monomer (1 mmol of **M1**, **M2**, **M3**, or **M4**) in 20 mL of dry $CHCl_3$ is added dropwise under fast stirring. The mixture is further stirred for 24, 48, or 72 h at room temperature under an Ar flow. The dark solution is poured into methanol (1 L), and the black precipitate is collected on a membrane filter. The precipitate is then immersed into a 1% v/v solution of hydrazine in methanol and stirred for 12 h. The polymer is then collected and washed with methanol. The polymer is than subsequently washed for 72 h by Soxhlet extractions with methanol and acetone, after which the soluble fraction is collected via extraction with $CHCl_3$ for 24 h. The $CHCl_3$ solution is then concentrated, and precipitation into methanol yields the polymer as a black, shining powder. The yields of the polymers are reported in Table 1.

Polymer P1. ^{1}H NMR ($CDCl_3$): 8.20−8.05 (br, 1H); 8.00−7.80 (br, 2H); 7.60−7.30 (br, 1H); 7.20−7.00 (br, 2H); 7.00−6.55 (br, 2H); 4.22−3.75 (br, 4H); 2.02−1.00 (br, 16H); 1.00−0.68 (br, 18H). Anal. Calcd for $C_{40}H_{50}N_2O_2S_2$: C 73.36; H 7.70; N 4.28; O 4.89; S 9.77. Found: C 72.45; H 8.22; N 3.76; O 5.15; S 9.13.

Polymer P2. ^{1}H NMR ($CDCl_3$): 8.20−8.05 (br, 1H); 8.00−7.80 (br, 1H); 7.60−7.30 (br, 1H); 7.20−7.00 (br, 2H); 7.00−6.55 (br, 1H); 4.22−3.75 (br, 4H); 2.98−2.28 (br, 4H); 2.02−1.00 (br, 36H); 1.00−0.68 (br, 24H). Anal. Calcd for $C_{56}H_{82}N_2O_2S_2$: C 76.49; H 9.41; N 3.19; O 3.64; S 7.28. Found: C 76.01; H 9.68; N 3.28; O 3.59; S 7.39.

Polymer P3. ^{1}H NMR ($CDCl_3$): 8.2 (br m, 2H), 7.1 (br m, 2H), 4.3 (br m, 8H), 4.1 (br m, 4H), 1.9 (br m, 2H), 1.6 (br m, 6H), 1.4−1.0 (br m, 12), 0.9 (br s, 6H), 0.8 (br s, 12H). Anal. Calcd for $C_{44}H_{54}N_2O_6S_2$: C 68.54; H 7.07; N 3.64; O 12.46; S 8.30. Found: C 67.17; H 7.49 N 3.24; O 12.92; S 7.52.

Polymer P4. ^{1}H NMR ($CDCl_3$): As this polymer comes from a polymerization of a mixture of four isomers, the material has a very complex spectrum.[21] Anal. Calcd for $C_{72}H_{110}N_2O_6S_2$: C 74.30; H 9.54; N 2.41; O 8.25; S 5.50. Found: C 73.15; H 10.12; N 1.99; O 8.97; S 4.70.

III. Results and Discussion

Monomer Synthesis. Among the approaches to low band gap polymers, the donor−acceptor route has received significant attention.[11] The central concept forming the basis of this route is that the interaction between a strong electron donor (D) and a strong electron acceptor (A) gives rise to an increased double bond character between these units, since they can accommodate the charges that are associated with such a mesomerism (D−A $\leftrightarrow$ D^+=A^-). Hence, a conjugated polymer with an alternating sequence of the appropriate donor and acceptor units in the main

Scheme 1. Synthesis of the Monomers M1−M4

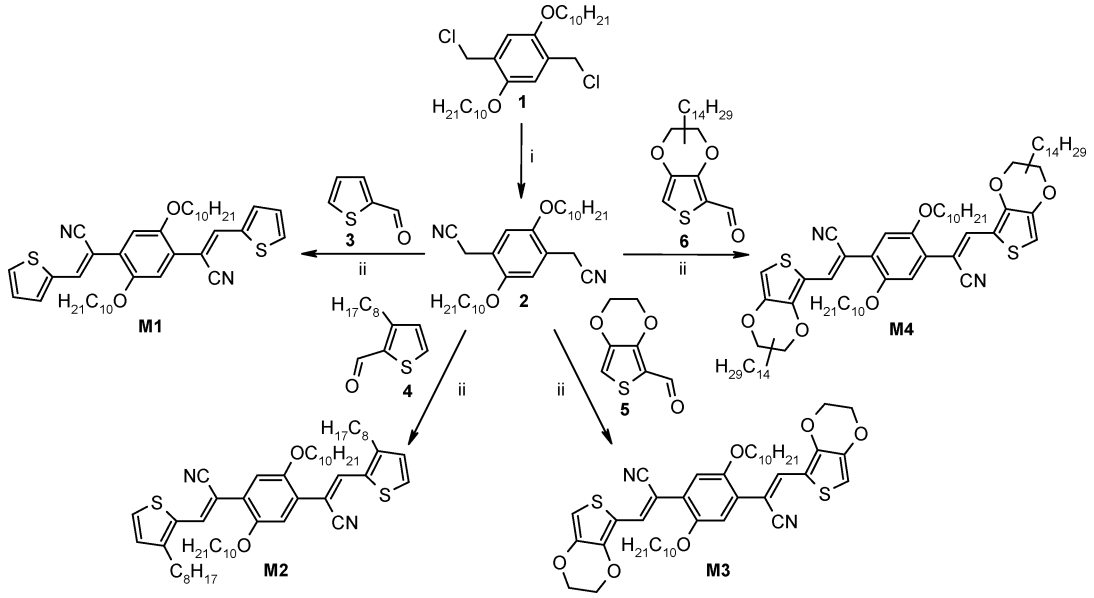

chain may show a decreased band gap. The aryl unit with a cyanogroup is among the most widespread electron-withdrawing groups in organic chemistry and can be easily obtained by applying a Knoevenagel condensation[12,22] of a thiophene carboxaldehyde (**3**, **4**, **5**, and **6**) with an aromatic acetonitrile moiety (**2**) in refluxing methanol containing sodium *tert*-butoxide, as shown in Scheme 1. The thiophene carboxaldehydes were either commercially available or prepared via a Vilsmeier formylation of the respective thiophene derivatives. The aromatic acetonitrile was prepared from 1,4-bischloromethyl-2,5-bis[3′,7′-dimethyloctyl)oxy]benzene (**1**) via nucleophilic substitution with sodium cyanide in DMF. The overall yields for the monomers were ranging between 40 and 60%. By this synthesis method four monomers were prepared whose structures consist of a central dialkoxyphenylene core para-disubstituted by two thiophene derivatives through a cyanovinylene linker. The long alkoxy chains on the central core enhance the solubility of the final polymer. By keeping both the central core and the acceptor strength constant, the influence of thiophenes with different donor characteristics was studied. Furthermore, the influence of extra solubilizing chains on the thiophene part was studied.

Polymerization. The polymers were prepared by chemical oxidation of the monomers using $FeCl_3$ according to a procedure similar to that of Sugimoto et al.[17] (Scheme 2). This method is very useful to prepare polythiophenes due to its simplicity and the high molecular weights achieved. To improve the reproducibility of the polymerizations, anhydrous $FeCl_3$ was freshly prepared from commercial $FeCl_3$ according to a described procedure.[18]

Polymerization of the monomers has been performed using three different reaction conditions (Table 1), deviating in the reaction times employed. The reaction proceeds with the formation of an initial dark-blue color and a subsequent black precipitate. After the polymerization, the polymers contain residual iron(III) salts which can be reduced in concentration with rigorous purification. A first precipitation in MeOH and subsequent in MeOH/hydrazine not only removes residual $FeCl_3$, but the latter also dedopes the polymers. Further traces of iron(III) salts are removed by Soxhlet extraction with methanol. During this step the polymer is also purified from unreacted monomer. Further extraction with acetone removes oligomeric and low molecular weight fractions from the polymers, and the

Scheme 2. Polymerization Reaction toward the Polymers P1−P4

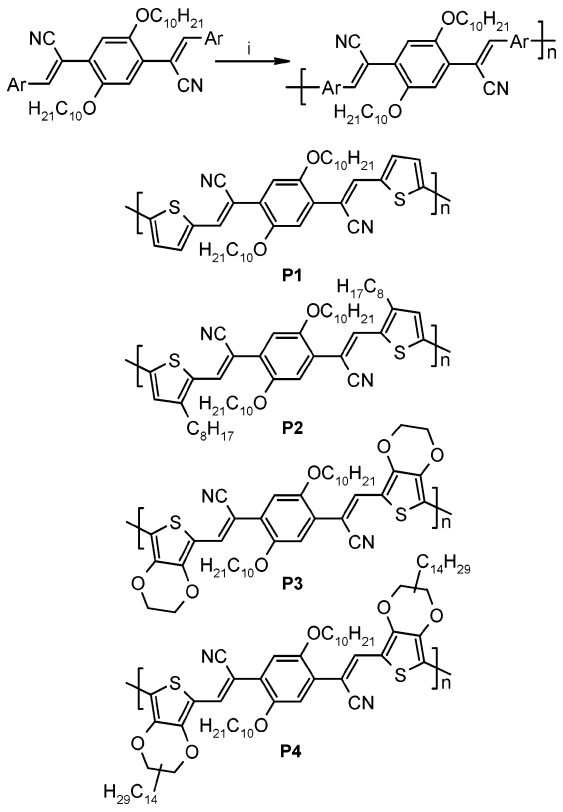

soluble fraction was eventually collected by extraction with chloroform. Polymerization results are shown in Table 1 where the characteristics of the different polymers from the different polymerizations are summarized. The weight-average molecular weights (M_w), the number-average molecular weights (M_n), and molecular weight distribution (PD) of the polymers have been determined by analytical SEC in THF using polystyrene standards. The reported overall yields (Y1) were determined after extraction with acetone, and the soluble polymer yield (Y2) indicates the soluble fraction of the polymer in chloroform.

It is clear that, for all the polymers, longer reaction times are causing lower molecular weights and lower overall yields (Y1).

Table 2. Optical Data of the Polymers P1−P4 Measured Both as Thin Film and in $CHCl_3$ Solution

	film			$CHCl_3$ solution		
	λ_{max} [nm]	λ_{onset} [nm]	E_g [eV][a]	λ_{max} [nm]	λ_{onset} [nm]	E_g [eV][a]
P1	520	700	1.77	500	650	1.91
P2	540	720	1.72	490	600	2.10
P3	630	780	1.59	580	710	1.75
P4	570	720	1.72	560	680	1.82

[a] Calculated from the intersection of the tangent on the low energetic edge of the absorption spectrum with the abscissa.

This is probably due to the presence of HCl in the reaction medium, although most of the HCl, formed during the reaction, is removed. The small amount that is left, in combination with very long reaction times induces degradation of the polymer chains, yielding highly dispersed, low molecular weight polymers. Our attempt to increase the solubility of the polymers by introduction of long alkyl side chains (**P2** and **P4**) was successful, as indicated by the high soluble polymer yield (Y2) comprised between 80 and 93%. Another interesting fact for these alkyl-substituted polymers (**P2** and **P4**) is that the molecular weights are much lower and the overall yields much higher than for the non-alkylated polymers (**P1** and **P3**). The sterical hindrance induced by the alkyl side chains on the thiophene units makes the monomers less reactive and causes the lower molecular weights.

The following characterization of electronic properties has been carried out on the samples prepared with a polymerization time of 24 h, since they have the highest molecular weights and the lowest polydispersities.

Optical Absorption. The electronic absorption data of the various polymers are listed in Table 2. All spectroscopic properties were measured both as thin film on quartz (Figure 1a) and in chloroform solution (Figure 1b).

Figure 1a shows that the absorption maximum (λ_{max}) of **P2** exhibits a 20 nm red shift as compared to **P1**. This shift is also observed for the band gap. The low energetic edge of the absorption spectrum of **P1** is at 700 nm, which corresponds to a band gap of 1.77 eV, while for **P2** the absorption onset is at 720 nm, corresponding to a band gap (E_g) of 1.72 eV. This behavior is a result of the electron-releasing effect of the octyl chains. Apparently, the electronic substituent effect created by the introduction of the alkyl side chains is larger than the possible effect of reduced electronic interchain interactions as well as the increased disorder in the conjugated system due to sterical hindrance imparted by the octyl side chains. The effect of sterical hindrance can be seen in **P3** when compared to **P4**. Here the red shift is 60 nm. This is due to the larger interchain distances imposed by the tetradecyl substituents attached at an sp^3 carbon which leads to a bigger decrease of π stacking interactions in the solid state. When comparing **P3** with **P1**, **P3** shows a bathochromic shift of 100 nm compared to **P1**, and the band gap of **P3** is 0.2 eV lower than the band gap of **P1**. Here, as is also observed by comparing the optical data of poly(thiophene) (λ_{max} = 480 nm, E_g = 1.9 eV) with poly(3,4-ethylenedioxythiophene) (λ_{max} = 610 nm, E_g = 1.6 eV), the strong electron-releasing ethylenedioxy groups in **P3** are causing this shift.

Because of the absence of π stacking in solution (Figure 1b, Table 2), overall, the λ_{max} and λ_{onset} values were lower than in the solid state although all trends mentioned above are also observed in solution. For **P4**, when measured in solution the optical spectrum remains practically identical to the one measured in film, with however a small (ca. 10 nm) hypsochromic shift of the absorption maximum. This again confirms that for **P4** almost no additional π stacking interaction is observed when going from solution to a thin film.

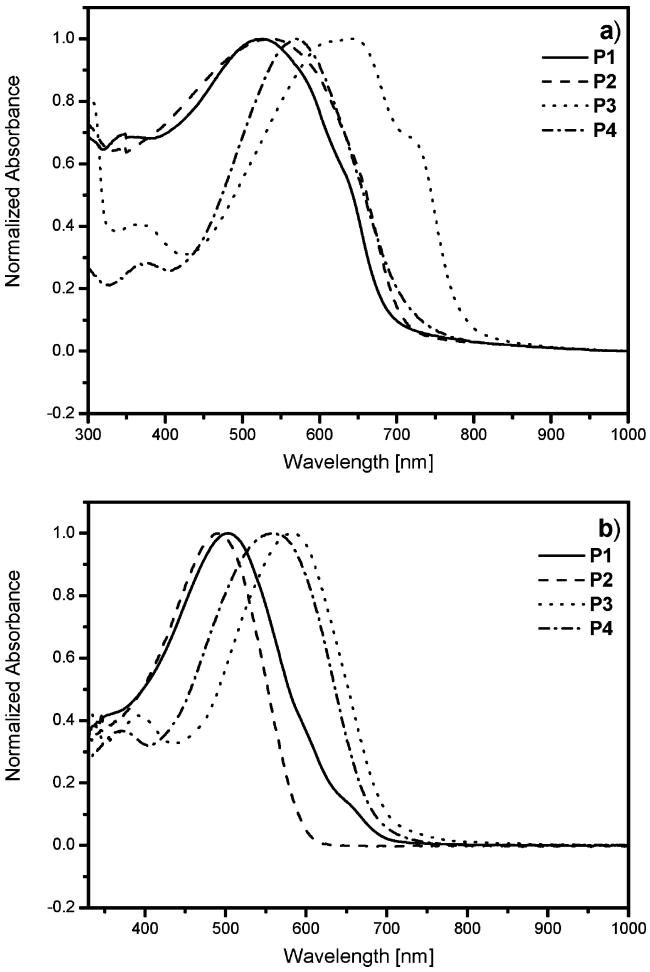

Figure 1. Normalized UV−vis absorption spectra of **P1**−**P4** as thin film (a) and in $CHCl_3$ solution (b).

Overall, as we expected, all four polymers show low band gaps, and by increasing the electron-releasing effect, the band gap of the polymers decreases from **P1** > **P2** > **P3**. For **P4** the introduction of alkyl substituents (although electron-releasing) give rise to a higher band gap compared to **P3**. It is noteworthy that no significant degradation of the conjugated system is observed in the temperature-dependent UV−vis spectrum during the heating process until 225 °C. Notwithstanding, thermal stability of the conjugated system up to 225 °C[23,24] is sufficiently high for potential device applications.

Electrochemistry. Cyclic voltammetry (CV) using 0.1 M $TBAPF_6$ as a supporting electrolyte in anhydrous ACN was employed to study the electrochemical behavior of the polymers and to estimate their highest occupied molecular orbital (HOMO) and lowest unoccupied molecular orbital (LUMO) energy levels. The cyclic voltammograms display quasi-reversible oxidation and reduction processes (Figure 2) for all the polymers. Therefore, electrochemically determined band gaps derived from the difference between onset potentials ($E_g = E^{ox}_{onset} - E^{red}_{onset}$) for oxidation and reduction of polymers can be deduced.

The CV data of the various polymers are gathered in Table 3. With an ethylenedioxy group incorporated (**P3**), a decrease in band gap of ca. 0.7 eV was found on going from **P1** to **P3**. As expected, the reduction potentials are hardly affected by the incorporation of the ethylenedioxy groups. This suggests that

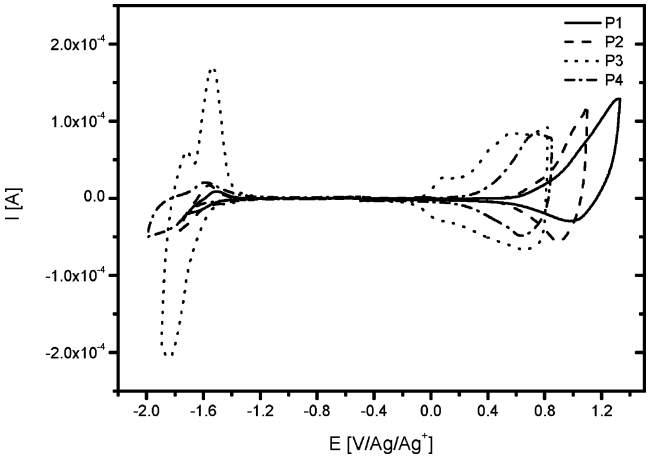

Figure 2. Cyclic voltammograms of the oxidation and reduction behavior of thin films of **P1**−**P4**.

Table 3. Electrochemical Data of the Polymers P1−P4

	E^{ox}_{onset}[V]	E^{red}_{onset}[V]	HOMO [eV]	LUMO [eV]	E_g [eV]
P1	+ 0.850	−1.460	−5.73	−3.42	2.31
P2	+ 0.573	−1.553	−5.48	−3.35	2.13
P3	+ 0.044	−1.600	−4.82	−3.27	1.55
P4	+ 0.402	−1.630	−5.34	−3.30	2.04

the reduction is mainly dominated by the presence of the cyanovinylene linkages and that for these polymers the variations in the band gap are mainly determined by the HOMO of the polymers. The effect of alkyl chain substitution on the oxidation and reduction process of the polymers can also be compared by using the values reported in Table 3.

The octyl substitution in **P2** decreases the oxidation potentials as compared with the nonsubstituted analogue **P1** as a result of the increased electron-donating effect by the octyl chain. It should be noted that the oxidation process can also be observed visually. A color change of the films from blue to light yellow was observed upon oxidation. Subsequently, in the reverse process upon dedoping the color of the film returned to blue. This observation further confirms the reversibility of the p-doping process. It is clear now from these results that changing of the substituents on the thiophene unit allows the modulation of the HOMO/ionization potential. This should be useful to enhance the absorption of photons in the active layer of an organic solar cell and efficient charge collection at the electrodes. Figure 3 exhibits the resulting energy band diagram in relation to the relative energy levels of the most frequently employed acceptor in organic solar cells, PCBM, and the workfunction of indium tin oxide (ITO) and aluminum (Al), which are usually applied as electrodes in polymer solar cells. The HOMO of the polymers **P3** and **P4** is distinctively higher in energy than that of PCBM. However, not the HOMO energy levels but the relative positions of the donor LUMO and the acceptor LUMO are important for the intended charge transfer. The difference between the LUMO's of **P1**−**P4** and PCBM is in the range of 0.6 eV, which is sufficiently high to enable an unrestricted and directed charge transfer.

Charge-Transfer Processes. PL and LI-EPR measurements were performed to examine the charge-transfer efficiency in blends of these polymers (acting as a donor) with PCBM (acting as an acceptor). **P2** was used as a model system for these measurements. Evidence for charge transfer from the polymer to the PCBM in the **P2**/PCBM blend is found in LI-EPR measurements, as shown in Figure 4. After illumination, the $PCBM^-$ signal is observed, and there is a clear increase of the

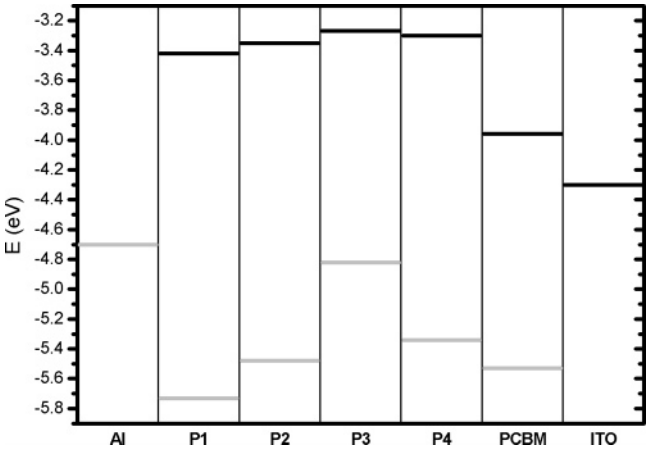

Figure 3. Energy band diagram with HOMO/LUMO levels of **P1**−**P4** and PCBM in relation to the work function of the common electrode materials ITO and Al.

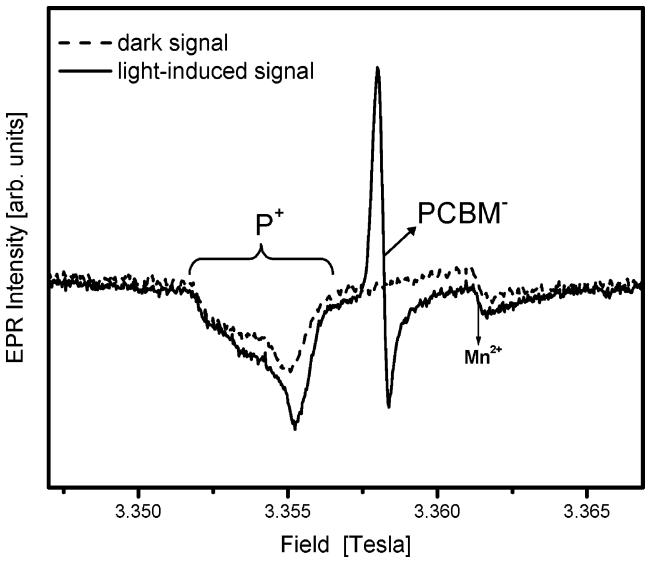

Figure 4. EPR spectra (dark and light-induced) of the **P2**/PCBM blend showing the positive polaron (P^+) and the $PCBM^-$ radical (T = 100 K, λ_{exc} = 488 nm). The unusual line shape of the P^+ signal results from the fast passage effect.[25] The Mn line indicated in the figure is originating from the cavity.

polaron (P^+) signal—note that the dark polaron signal is attributed to residual impurities present in the polymer despite the rigorous purification. The g values of both the polaron and the PCBM correspond closely to those observed for an MDMO-PPV/PCBM blend.[25]

The occurrence of charge transfer is confirmed by the quenching of the PL emission (by a factor of 35) when going from the **P2** to the **P2**/PCBM film (Figure 5a) and, correspondingly, with the drastic decrease of the decay time (Figure 5b). It should be mentioned that the PL efficiency, even in the pure **P2** polymer film, is much lower than usually observed in MDMO-PPV. This points to a competition with an efficient nonradiative decay process. Further, one notices the large Stokes shift between the absorption maximum of the **P2** film and the PL emission (∼200 nm compared to a Stokes shift of ∼100 nm for MDMO-PPV). Correspondingly, there is a large shift between the **P2** emission in solution and in film, a shift which is also not observed for the conventional polymers like MDMO-PPV. This relatively large Stokes shift indicates an important configurational relaxation in the excited state.

Solar Cells. Typical $I-V$ characteristics of ITO/PEDOT:PSS/**P2**:PCBM/LiF/Al (named **P2** device) and ITO/PEDOT:PSS/

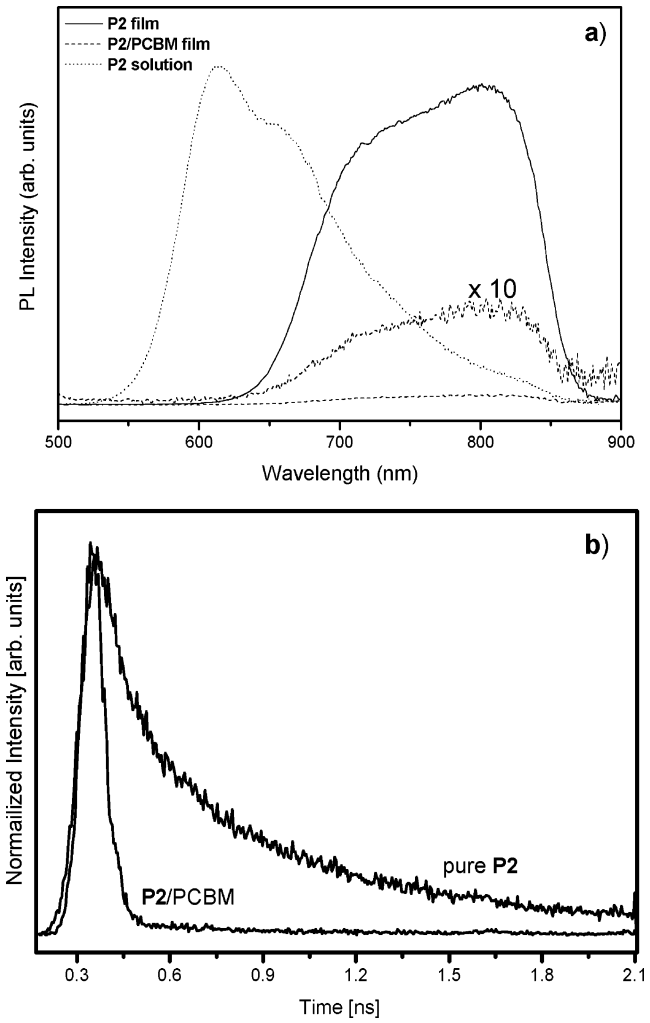

Figure 5. (a**)** Photoluminescence spectra of **P2** in $CHCl_3$ solution and of thin spin-coated films of **P2** and of the blend **P2**/PCBM. For clarity, the magnified signal (×10) from the **P2**/PCBM film is shown as well. (b**)** Time decay (normalized) of the PL emission of **P2** and **P2**/PCBM films. The **P2** film shows a double-exponential decay with times $\tau_1 = \sim 130$ ps and $\tau_2 = \sim 700$ ps. The decay of the **P2**/PCBM blend is resolution limited by the response of the streak camera detector.

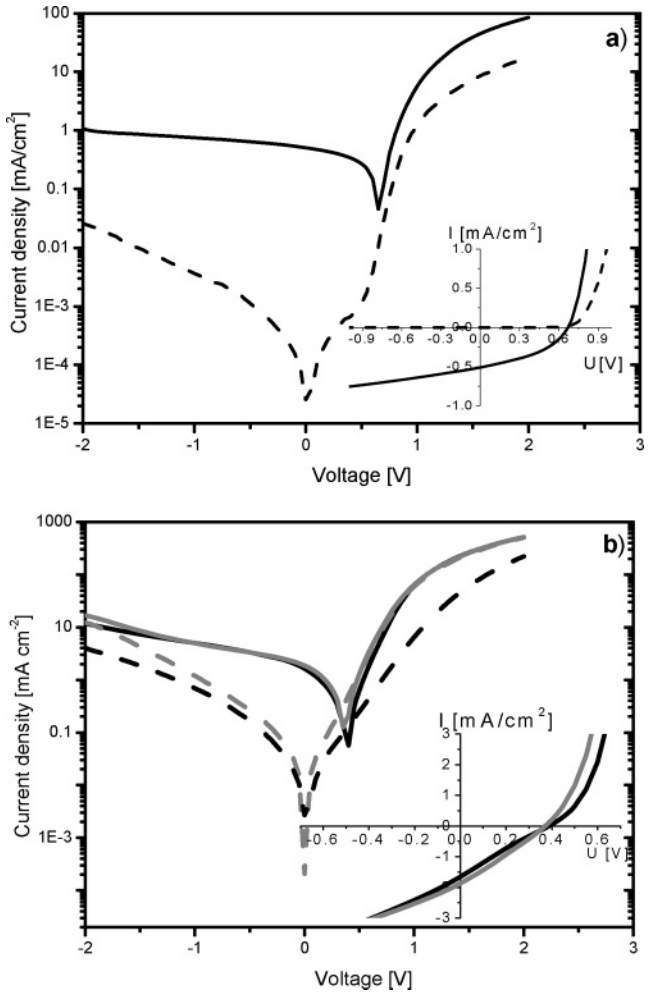

Figure 6. Semilogarithmic and linear (inset) representations of $I-V$ characteristics (AM 1.5, 100 mW/cm^2) of (a**)** ITO/PEDOT:PSS/**P2**:PCBM/LiF/Al and (b**)** ITO/PEDOT:PSS/**P3**:PCBM/LiF/Al cells before (black line) and after (gray line) annealing. The solid line represents data obtained under illumination, while the dashed line is measured in the dark.

P3:PCBM/LiF/Al (named **P3** device) devices are shown, both in the dark (dashed line) and under AM 1.5 illumination (solid line), in parts a and b of Figure 6, respectively. The **P2** device performance shows open circuit voltages (V_{OC}) of 650 mV, short circuit currents (I_{SC}) of 0.5 mA/cm^2, fill factors (FF) of 0.42, and a conversion efficiency (η) of about 0.14%, while the **P3** device exhibits lower V_{OC} (400 mV), lower FF (0.22), but much higher I_{SC} (1.64 mA cm^{-2}), leading to the same value of $\eta =$ 0.14%. Optimization of the device parameters by thermal annealing shows a slight increase in the final photovoltaic performance for the **P3** device with the following characteristics: $V_{OC} = 350$ mV, $I_{SC} = 1.87$ mA cm^{-2}, and FF = 0.29 (gray line in Figure 6b), which results in $\eta = 0.19\%$, while annealing has not shown an improved effect on the **P2** device.

Figure 7 shows IPCE spectra (black solid lines) of the photovoltaic cells ITO/PEDOT:PSS/**P2**:PCBM/LiF/Al (a) and ITO/PEDOT:PSS/**P3**:PCBM/LiF/Al (b) with the normalized absorption of the corresponding pristine polymer films (gray solid lines).

The photocurrent spectrum of the **P2** device shows an onset at about 710 nm (1.75 eV) close to the optical band gap and exhibits a maximum of 3% at 600 nm (Figure 7a), while the IPCE spectrum for **P3** device extends its onset to higher wavelength at about 780 nm (1.54 eV) with a maximum absorption of more than 12% at 550 nm. **P3** possesses a quite low band gap ($E_g = 1.59$ eV), resulting in an increase in absorption of light. As a consequence, the I_{SC} increases but at the same time V_{OC} is lowered. The lower band gap of the polymer resulting from a decrease in the oxidation potential (i.e., increasing the HOMO level) may therefore reduce the V_{OC} because the V_{OC} of polymer/fullerene-based solar cells depends on the energy difference between the HOMO of the donor and the LUMO of the acceptor.[2]

The results for solar cell performance are disappointing in spite of both the lower band gap of the polymer and the efficient charge transfer in the blends with PCBM. Also, the electrochemical potentials are compatible with the requirements for this type of solar cell,[9] with reasonable V_{OC} values although lower than in optimal devices.

The low I_{SC} values observed for these devices eventually point to low mobility of the carriers. Indeed, the hole mobility in the pure polymer films measured in a field effect transistor was found below 10^{-6} cm^2/(V s) for all polymers.

IV. Conclusions

In conclusion, the synthesis of four different soluble low band gap polymers (1.6−2.0 eV) has been demonstrated. The

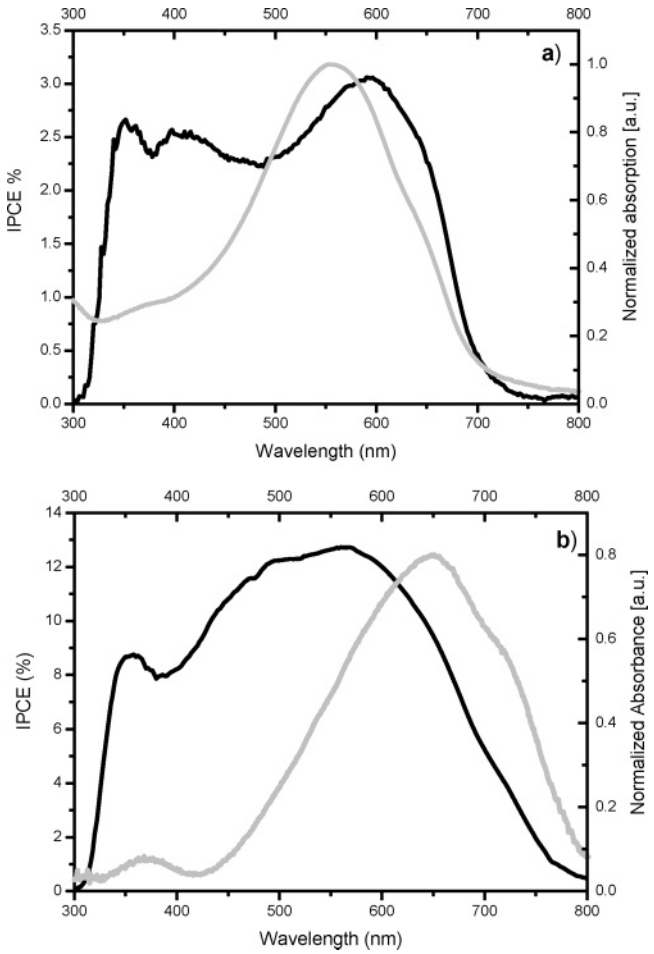

Figure 7. Photocurent spectrum (black solid line) of photovoltaic devices (a**)** ITO/PEDOT:PSS/***P2***:PCBM/LiF/Al and (b**)** ITO/PEDOT:PSS/**P3**:PCBM/LiF/Al and the normalized optical absorptions for the corresponding pristine polymers (gray solid line).

polymers were synthesized by $FeCl_3$ oxidative polymerization. The influence of time on the polymerization was studied. Long reaction times give rise to lower molecular weights and lower yields. The introduction of extra solubilizing chains (**P2** and **P4**) on the thiophene unit increases the solubility of the final polymers but also lowers their molecular weights as a result of steric hindrance during the polymerization. The influence of the electron donor strength of the thiophene units was studied with UV−vis absorption spectroscopy and cyclic voltammetry. It is shown clearly that in going from **P3** over **P2** to **P1** the HOMO increases due to a decrease of the electron donor strength in the polymer. As a result hereof the band gap increases. The introduction of alkyl substituents in **P4** give rise to a higher band gap. The reason for this behavior is related to the steric hindrance imparted by the tetradecyl substituents that affect the planarity of the molecule. In this work we were able to show that changing of the substituents on the thiophene unit allows the modulation of the HOMO/ionization potential. Efficient charge transfer is demonstrated in blends of **P2** with PCBM by PL and LI-EPR measurements. However, solar cells made of the polymers showed only low efficiencies, which is related to the low hole mobilities observed in the pure polymer films.

Acknowledgment. The authors gratefully acknowledge the Belgian Programme on Interuniversity Attraction Poles (IUAP), initiated by the Belgian State Prime Minister's Office, for the financial support. We also thank the IWT (Institute for the Promotion of Innovation by Science and Technology in Flanders) for the financial support via the SBO-project 030220 "Nanosolar" and the European FP6-MOLYCELL project Contract SES6-CT-2003-502783. K.C. thanks the IUAP-V for granting a PhD fellowship and Dr. Marinella Catellani for her help and discussion on the oxidative polymerization. S.F. thanks the BOF-UHasselt for granting a PhD fellowship.

Supporting Information Available: ^{1}H NMR raw spectra of monomer **M4** and polymer **P4**. This material is available free of charge via the Internet at http://pubs.acs.org.

References and Notes

(1) Halls, J. J. M.; Walsh, C. A.; Greenham, N. C.; Marseglia, E. A.; Friend, R. H.; Moratti, S. C.; Holmes, A. B. *Nature (London)* **1995**, *376*, 498−500.

(2) Brabec, C. J.; Sariciftci, N. S.; Hummelen, J. C. *Adv. Funct. Mater.* **2001**, *11*, 15−26.

(3) Hoppe, H.; Sariciftci, N. S. *J. Mater. Res.* **2004**, *19*, 1924−1945.

(4) Dennler, G.; Sariciftci, N. S. *Proc. IEEE* **2005**, *93*, 1429−1439.

(5) Munters, T.; Martens, T.; Goris, L.; Vrindts, V.; Manca, J.; Lutsen, L.; De Ceuninck, W.; Vanderzande, D.; De Schepper, L.; Gelan, J.; Sariciftci, N. S.; Brabec, C. J. *Thin Solid Films* **2002**, *403*, 247−251.

(6) Hoppe, H.; Egbe, D. A. M.; Muhlbacher, D.; Sariciftci, N. S. *J. Mater. Chem.* **2004**, *14*, 3462−3467.

(7) Winder, C.; Sariciftci, N. S. *J. Mater. Chem.* **2004**, *14*, 1077−1086.

(8) Henckens, A.; Colladet, K.; Fourier, S.; Cleij, T. J.; Lutsen, L.; Gelan, J.; Vanderzande, D. *Macromolecules* **2005**, *38*, 19−26.

(9) Scharber, M. C.; Mühlbacher, D.; Koppe, M.; Denk, P.; Waldauf, C.; Heeger, A. J.; Brabec, C. J. *Adv. Mater.* **2006**, *18*, 789−794.

(10) Reyes-Reyes, M.; Kim, K.; Dewald, J.; Lopez-Sandoval, R.; Avadhanula, A.; Curran, S.; Carroll, D. L. *Org. Lett.* **2005**, *7*, 5749−5752.

(11) van Mullekom, H. A. M.; Vekemans, J. A. J. M.; Havinga, E. E.; Meijer, E. W. *Mater. Sci. Eng., R* **2001**, *32*, 1−40.

(12) Sotzing, G. A.; Thomas, C. A.; Reynolds, J. R.; Steel, P. J. *Macromolecules* **1998**, *31*, 3750−3752.

(13) Wagner, P.; Aubert, P.-H.; Lutsen, L.; Vanderzande, D. *Electrochem. Commun.* **2002**, *4*, 912−916.

(14) Seshadri, V.; Sotzing, G. A. *Chem. Mater.* **2004**, *16*, 5644−5649.

(15) Thomas, C. A.; Zong, K. W.; Abboud, K. A.; Steel, P. J.; Reynolds, J. R. *J. Am. Chem. Soc.* **2004**, *126*, 16440−16450.

(16) van Breemen, A.; Issaris, A.; de Kok, M.; Van der Borght, M.; Adriaensens, P.; Gelan, J.; Vanderzande, D. *Macromolecules* **1999**, *32*, 5728−5735.

(17) Sugimoto, R.; Takeda, S.; Gu, H. B.; Yoshino, K. *Chem. Express* **1986**, *1*, 635.

(18) Pray, A. R. In *Inorganic Synthesis*; Moeller, T., Ed.; McGraw-Hill Book Co.: New York, 1957; Vol. 5, pp 153−155.

(19) Colladet, K.; Nicolas, M.; Goris, L.; Lutsen, L.; Vanderzande, D. *Thin Solid Films* **2004**, *451*−*52*, 7−11.

(20) Note: ^{1}H NMR raw spectrum of **M4** is shown in the Supporting Information.

(21) Note: ^{1}H NMR raw spectrum of **P4** is shown in the Supporting Information.

(22) Moratti, S. C.; Cervini, R.; Holmes, A. B.; Baigent, D. R.; Friend, R. H.; Greenham, N. C.; Gruner, J.; Hamer, P. J. *Synth. Met.* **1995**, *71*, 2117−2120.

(23) Note: It is our experience that the thermal stability of conjugated polymers is limited by the stability of the conjugated system rather than by the thermal stability of the polymer itself. For a detailed study of the stability of the conjugated system measured with an in-situ UV−vis technique, we refer to ref 24.

(24) Kesters, E.; Vanderzande, D.; Lutsen, L.; Penxten, H.; Carleer, R. *Macromolecules* **2005**, *38*, 1141−1147.

(25) De Ceuster, J.; Goovaerts, E.; Bouwen, A.; Hummelen, J. C.; Dyakonov, V. *Phys. Rev. B* **2001**, *64*, 195206.

MA061760I